Preparation and characterization of multicomponent porous materials prepared by the sol-gel process

**E. Minor-Pérez · R. Mendoza-Serna · J. Méndez-Vivar ·
R. C. Pless · D. Quintana-Zavala · R. Torres-Robles**

Abstract An experimental strategy was developed to obtain transparent Si-Al-Ti-Ni-Mo and Si-Zr-Ti-Ni-Mo sols via the sol-gel process. The sol was prepared from $Si(OEt)_4$ (TEOS), $Al(OBu^s)_3$ (OBu^s: $C_2H_5CH(CH_3)O$), $Ti(OEt)_4$ (OEt: OCH_2CH_3), $Zr(OPr^n)_4$ (OPr^n: $OCH_2CH_2CH_3$). In both cases nickel nitrate hexahydrate ($Ni(NO_3)_2 \cdot 6H_2O$) and ammonium heptamolybdate tetrahydrate (($NH_4)_6Mo_7O_{24} \cdot 4H_2O$) were the Ni and Mo sources, respectively. The sols were characterized by Fourier Transform Infrared Spectroscopy (FTIR). Assignments of the simultaneous formation of the Si-O-Al, Si-O-Ti, Si-O-Ni, and Si-O-Zr bonds were done. The sols were polymerized at room temperature (293 K) to obtain gels, and these were dried at 423 K and calcined at 573, 853 and 893 K in air. The characterization techniques used were small-angle X-ray scattering (SAXS), X-ray diffraction (XRD), scanning electron microscopy (SEM), and ^{29}Si and ^{27}Al magic angle spinning nuclear magnetic resonance (MAS NMR). The density of the solids was measured following ASTM method D-4892 and the porosity and surface area were determined by N_2 adsorption/desorption isotherms. The corresponding average pore diameters were evaluated using the BJH, HK, and DA methods.

Present address:
Facultad de Estudios Superiores Zaragoza, U.N.A.M., Batalla del 5 de Mayo s/n esq. Fuerte de Loreto, Col. Ejército de Oriente, México D. F., 09230, México

E. Minor-Pérez (✉) · D. Quintana-Zavala
CICATA-IPN, Unidad Legaria, México, D.F., 11500, Mexico
e-mail: mypes6@yahoo.com.mx

R. Mendoza-Serna
FES-Zaragoza, UNAM, México, D.F., 09230, Mexico

J. Méndez-Vivar
Universidad Autónoma Metropolitana-Iztapalapa, Depto. de Química, A.P. 55-534, México, D.F., 09340, Mexico

R. C. Pless
CICATA-IPN, Unidad Querétaro, Qro., 76040, Mexico

R. Torres-Robles
Instituto Mexicano del Petróleo, Programa de Ingeniería Molecular, México D.F., 07730, Mexico

Introduction

In recent decades, the synthesis and characterization of multicomponent materials has increased very rapidly [1]; the sol-gel processing has received increased attention due to its ability to produce high ceramic powders, coatings, and glasses [2, 3]. Mixed oxide supports containing Mo and W active components and Co or Ni promoters have been studied for hydrodesulfurization, hydrogenation, hydrodenitrogenation and hydrodeoxigenation in the oil industry. The TiO_2-Al_2O_3 system has been extensively studied because of its commercial prospects; SiO_2-Al_2O_3 and ZrO_2-TiO_2 also have received considerable attention due to support effects in dispersing the active components and promoters and altering the metal-support interaction [4]. The homogeneous incorporation of Ti and Zr into an SiO_2 matrix is important to obtain materials that exhibit chemical, thermal, and mechanical stability. These properties are essential in applications such as thin films, catalytic membranes, and catalytic supports [5–11]. The sol-gel method offers several advantages such as high purity of the final material, microstructure control, homogeneity on the molecular scale, and low-temperature preparation [12]. To ensure the

homogeneity of the Si-Al-Ti-Ni-Mo and Si-Zr-Ti-Ni-Mo sols we have taken into account several key points of the sol-gel process.

1. The hydrolysis rate of aluminum, titanium, and zirconium alkoxides are much faster than that of TEOS. The differences in structure and bond chemistry among these alkoxides (Si, Al, Ti, Zr) requires a procedure of hydrolysis and condensation of the mixed sols to tailor the structure on the molecular scale.
2. The use of acetylacetone (acacH) as a stabilizing agent in the molar ratio acac:M, 2:1 (M: Al, Ti, Zr) to chelate the aluminum, titanium, and zirconium alkoxides.

AcacH has often been reported in the sol-gel literature as a modifying agent for $Al(OBu^s)_3$ [13–15], $Ti(OEt)_4$ [16], and $Zr(OPr^n)_4$ [17, 18]. The purpose of using such multicomponent systems is to combine the properties of all of the component oxides for use in simultaneous processes of separation-reaction. In hydrodesulfurization and hydrogenation reactions Mo exhibits catalytic activity and when it is combined with Ni the activity is dramatically increased. In the literature there are reported compositions of 3 wt.% Ni and 8 wt.% Mo as those where the catalytic activity is maximum on an alumina and alumina-titania mixed oxides supports [4]. In addition, using only titania as support the activity is enhanced. However, the titania support presents the disadvantage of a low surface area and poor thermal stability, compared to their alumina counterparts. The molar ratios of mixed oxides that have been studied are 50:50 TiO_2:Al_2O_3, 12:88 TiO_2-SiO_2 and 65:35 TiO_2:ZrO_2 giving as a result excellent catalytic activity with high surface area [10]. In order to obtain a material with high catalytic activity, high permeability and considerable selectivity, we prepared a microporous and mesoporous materials with these characteristics. As a result, catalytic membranes of multicomponent systems consisting of Si-Al-Ti-Ni-Mo and Si-Zr-Ti-Ni-Mo were prepared.

Experimental

Preparation of an A2 sol

The A2 sol was prepared by the HCl two-step catalyzed hydrolysis and condensation of tetraethoxysilane (TEOS, Aldrich, 98%). TEOS was dissolved in ethanol (EtOH, Baker) at room temperature and then H_2O and a 1 M HCl solution were added. The sol was stirred and heated at 333 K for 90 min, to produce a stock sol. The molar ratios TEOS:EtOH:H_2O:HCl were 1.0:3.8:1.0:7×10^{-4}. In the second step, more H_2O and HCl were added at room temperature, so that the final molar ratios TEOS:EtOH:H_2O:HCl

were 1.0:3.8:5.1:0.06, respectively. The A2 sol was aged 2 h at room temperature and then mixed with $Al_2Si_2O_5(OH)_4$ (kaolin, Aldrich), used as a molecular sieve to eliminate most of the H_2O molecules. The A2 sol was filtered and recovered [19].

Preparation of the Si-X-Ti-Ni-Mo sol (X: Al, Zr)

A solution composed of acacH in EtOH was added to a sol containing $Al(OBu^s)_3$ or $Zr(OPr^n)_4$ dissolved in EtOH. AcacH dissolved in EtOH was added to a previously prepared sol, composed of $Ti(OEt)_4$ in EtOH. The A2 sol was added dropwise to the chelating Ti sol (addition time: three hours). The Si-Ti sol was added dropwise to the chelating Al or Zr sol (addition time: four hours), to obtain the Si-X-Ti sol. The molar ratios Si-Al-Ti and Si-Zr-Ti were 50:25:25 and 50:17.5:32.5, respectively. Finally the $(Ni(NO_3)_2 \cdot 6H_2O)$ and $((NH_4)_6Mo_7O_{24} \cdot 4H_2O)$ were added to obtain the Si-X-Ti-Ni-Mo sol. The Ni and Mo content in the Si-Al-Ti-Ni-Mo and Si-Zr-Ti-Ni-Mo sols were 2.94 and 3.0 wt.% and 7.46 and 9.93 wt.%, respectively, taking into account the catalytic activity required [4]. All the reactions were performed at room temperature (298 K). The sols were transparent and stable during the whole polymerization process.

Characterization techniques

Small-angle X-ray scattering (SAXS) measurements were done with an equipment composed of a Kratky camera coupled to a copper anode tube. Nickel filters were employed to provide a wavelength selection which comprised a narrow band around the CuKα line. Small-angle X-ray curves were recorded with a position- proportional counter. Data were analyzed as suggested in refs. [20–22]. The FTIR spectra of the sols were obtained using a Perkin Elmer 1600 spectrophotometer in the 4000–400 cm^{-1} region using nujol as the solvent. The samples were deposited between KBr plates and then analyzed.

X-ray diffractograms were obtained using a D8 Discover equipment with zirconium-filtered molybdenum X-rays. High values of the angular parameter (s = 4Π sin θ/λ, where θ is the Bragg angle and λ the wavelength) were thus obtained. The intensity values were read at intervals $\Delta 2\theta = 1/8°$ from $2\theta = 5°$ to $2\theta = 70°$.

The scanning electron microscopy results were obtained using a scanning microscope XL30ESEM. Preparation of samples included deposition of a 1.0% formvar solution in ethylene dichloride film (Electron Microscopy Science) on Cu grids. The grids were coated with carbon by sputtering. A drop of a sonicated slurry prepared using EtOH to suspend the xerogel was poured over a coated grid and left to slowly dry overnight. An additional coating was done with carbon to

Table 1 FTIR bands assignment in fresh Si-Al-Ti-Ni-Mo and Si-Zr-Ti-Ni-Mo sols

Assignment	Wavenumber (cm⁻¹)	
	Si-Al-Ti-Ni-Mo	Si-Zr-Ti-Ni-Mo
COO- -M, M: Zr, Ti [25]		1563
		1532
Si-O-Al [26, 27]	1076	
Si-O stretch in linear Si-O-Si [25]		1074
Si-O-Ni [28]	1033	1030
Si-O-Ti [29, 30]	937	934
Mo-O-Mo [31]	806	
Si-O-Zr [25, 26, 30]		800
O-Mo-O [32]		546
Si-O-Si [33]		455

ensure that samples were electrically conductive and stable during analysis.

^{29}Si MAS NMR studies were performed for Si-Al-Ti-Ni-Mo and Si-Zr-Ti-Ni-Mo solid samples calcined at 893 K. ^{27}Al MAS NMR was performed for Si-Al-Ti-Ni-Mo sample. An Avance 400 Bruker spectrometer was used. Mea-

surements were done at 300 K. The ^{29}Si MAS NMR study was done at 7.5 KHz spinning speed. The Si resonance frequency was 79.4981655 MHz. The ^{27}Al study was done at 12 KHz spinning speed. The Al resonance frequency was 104.2660911 MHz.

The N_2 adsorption/desorption isotherms of the solids dried at 423 K and calcined at 573, 853 and 893 K, were measured at 77 K in a Micromeritics ASAP 2405 after outgassing at
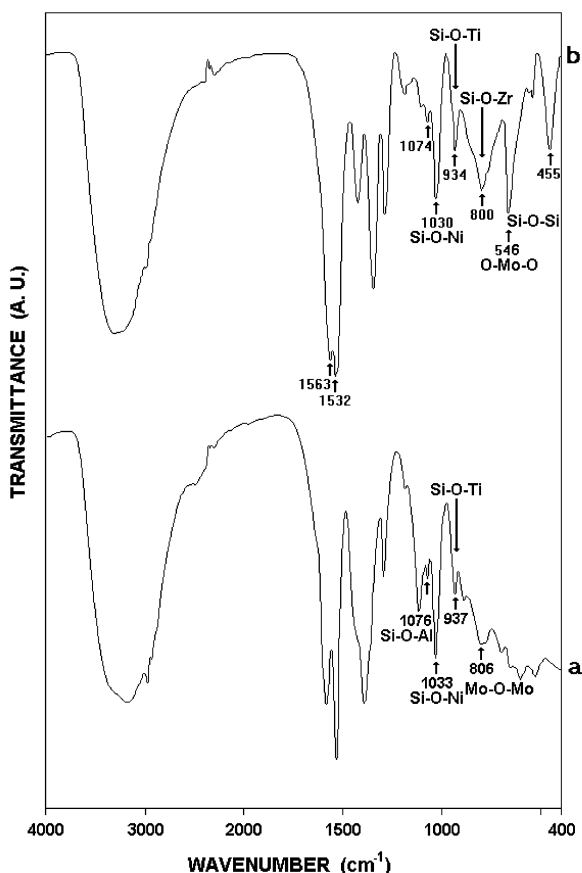

Fig. 1 FTIR spectra of fresh sols: (a) Si-Al-Ti-Ni-Mo and (b) Si-Zr-Ti-Ni-Mo
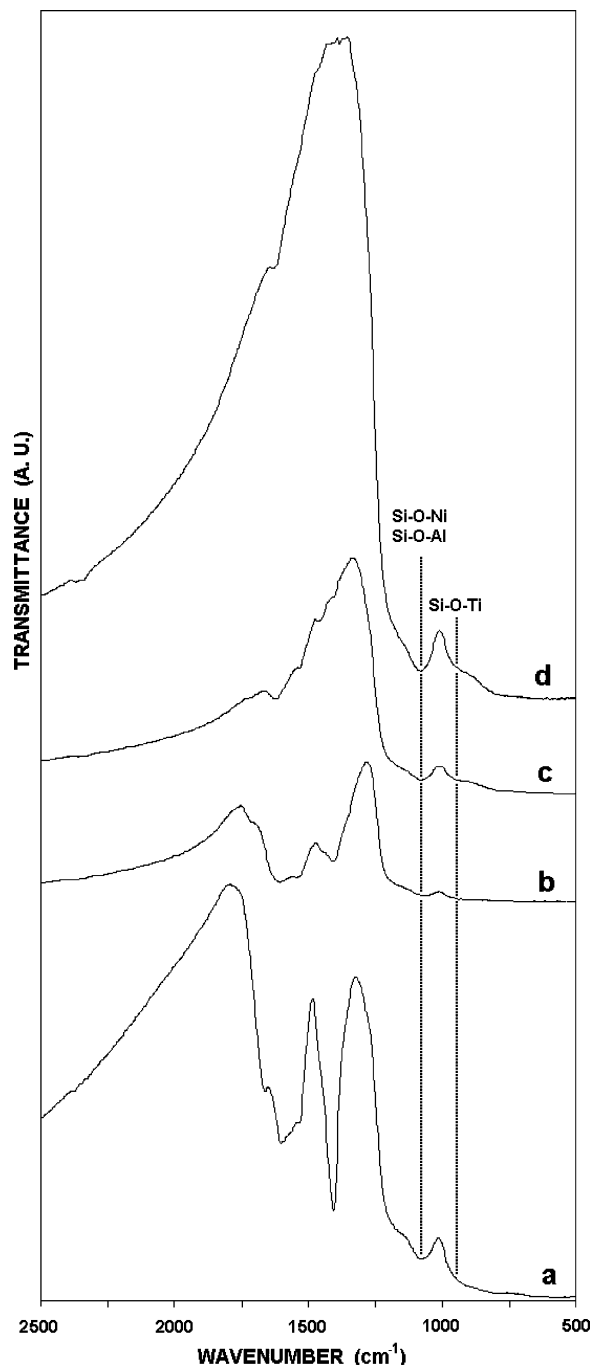

Fig. 2 FTIR spectra of Si-Al-Ti-Ni-Mo: (a) xerogel dried at 423 K, and calcined solids at: (b) 573 K, (c) 853 K and (d) 893 K

423 K for 12 h. Finally, the density of Si-Al-Ti-Ni-Mo and Si-Zr-Ti-Ni-Mo oxides was measured using a Micromeritics 1320 autopycnometer using He, following the ASTM method D-4892 on a sample previously dried at 383 K for 1 h to eliminate moisture.

Results and discussion

The SAXS results obtained from fresh Si-Al-Ti-Ni-Mo and Si-Zr-Ti-Ni-Mo sols indicated that the gyration radius (Rg) values were 13.0 nm and 9.8 nm, respectively, whereas the fractal dimensions (Df) were 2.0 and 1.8, respectively. These values indicate that Si-Al-Ti-Ni-Mo is a structure composed of randomly branched oligomers [23], while the Si-Zr-Ti-Ni-

Mo SAXS results indicate that mainly linear swollen polymers were obtained [24].

The FTIR bands assignment for the Si-Al-Ti-Ni-Mo and Si-Zr-Ti-Ni-Mo fresh sols is given in Table 1. The Si-O-Al, Si-O-Ni and Si-O-Ti bonds were detected at 1076, 1033 and 937 cm^{-1}, respectively, in the Si-Al-Ti-Ni-Mo spectra. The Si-O-Ni, Si-O-Ti and Si-O-Zr bonds were detected at 1030, 934 and 800 cm^{-1}, respectively, in the Si-Zr-Ti-Ni-Mo FTIR spectra. The spectra are shown in Fig. 1. In addition, the FTIR studies of xerogels and calcined oxides were performed in the region between 2500 and 500 cm^{-1}. The spectra for Si-Al-Ti-Ni-Mo xerogel and calcined oxide appear en Fig. 2. The most important feature in these spectra was the detection of the Si-O-Ni and Si-O-Al bands. The Si-O-Ni and Si-O-Al bands appeared overlapped between
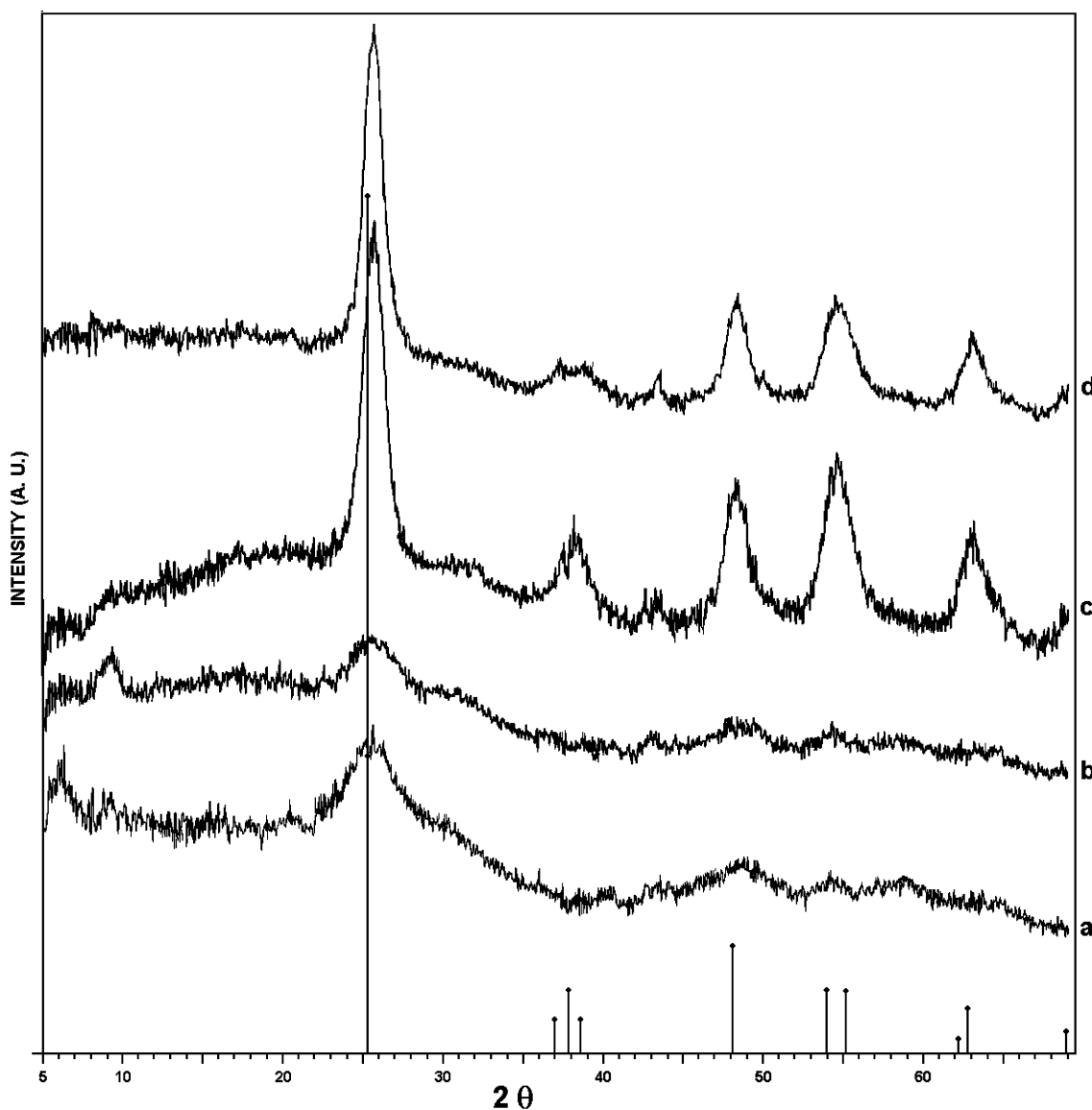

Fig. 3 X-ray powder diffraction patterns of Si-Al-Ti-Ni-Mo at: (a) 423, (b) 573, (c) 853, and (d) 893 K

1030 at 1080 cm^{-1} region and the Si-O-Ti band appears at 950 cm^{-1}. Similar results for the Si-O-Ni, Si-O-Ti and Si-O-Zr bands were obtained for the Si-Zr-Ti-Ni-Mo xerogel and calcined oxides.

The Si-Al-Ti-Ni-Mo and Si-Zr-Ti-Ni-Mo powders analyzed by X-ray diffraction were found to be amorphous even after thermal treatment at 573 K. The XRD patterns of the Si-Al-Ti-Ni-Mo powders are shown in Fig. 3. Weak reflection peaks due to anatase were identified only after calcining at 853 K. Similar results were obtained for the Si-Zr-Ti-Ni-Mo samples. According to these results the powders structure was amorphous up to 573 K.

The scanning electron microscopy image for Si-Al-Ti-Ni-Mo calcined at 893 K showed a bimodal size distribution, consisting of big and small faceted particles. The smaller particles are about 25 μm and the larger ones are 120 μm. For the Si-Zr-Ti-Ni-Mo, the smaller particles are 25 μm average size, and the larger ones are 175 μm. In both cases the morphology is well defined, showing different shapes, smooth and flat surfaces, faces and edges (image not shown here).

The results for the ^{29}Si MAS NMR spectra of the Si-Al-Ti-Ni-Mo and Si-Zr-Ti-Ni-Mo solids samples calcined at 893 K are presented in Fig. 4. In pure silicate, SiO$_4$ tetrahedra can exist in five states of coordination involving Si$-$O$-$Si bonds, each state designated by the symbol Q^n, where n is the degree of Si atom substitution. In order to compare the relative amounts of Q^1, Q^2, Q^3, and Q^4 species, we considered the chemical range -80 to -89.9 ppm for Q^1, -90 to -99 ppm for Q^2, -99.1 to -108.9 ppm for Q^3 and -109 to -120 ppm for Q^4, as in Ref. [34]. The incorporation of Al^{+3} or Zr^{+4} into the Si-X-Ti-Ni-Mo systems considerably modifies the solid structure as can be seen in Fig. 4. The Q distribution turns out to be quite different, the difference can be attributed to the electronegativity and coordination number of the cation, Al^{+3} or Zr^{+4}. Besides, ^{27}Al nuclei also provide an excellent tool to distinguish the coordination number of the Al species in the solid state [35], shown above of the same figure. The chemical shift of the ^{27}Al nucleus is very sensitive to the coordination number with oxygen. The resonance of tetracoordinated aluminum (Al^{IV}) sites appears between 55 and 70 ppm, the pentacoordinated Al atoms (Al^{V}) is observed between 25 and 35 ppm and the hexacoordinated Al atoms (Al^{VI}) between 0 and 11 ppm [36]. The ^{27}Al MAS NMR spectrum of the Si-Al-Ti-Ni-Mo sample calcined at 893 K, shows tetracoordinated, pentacoordinated and hexacoordinated Al sites are already present [37].

The isotherms for the Si-Al-Ti-Ni-Mo at 423 K and 893 K appear in Fig. 5. The samples exhibit a type I isotherm [38, 39], indicating that micropores are present along with mesopores. The solids calcined at 853 and 893 K exhibit a type H2 hysteresis loop. In these cases the pore size distribution and shape is not well defined [40]. The corresponding
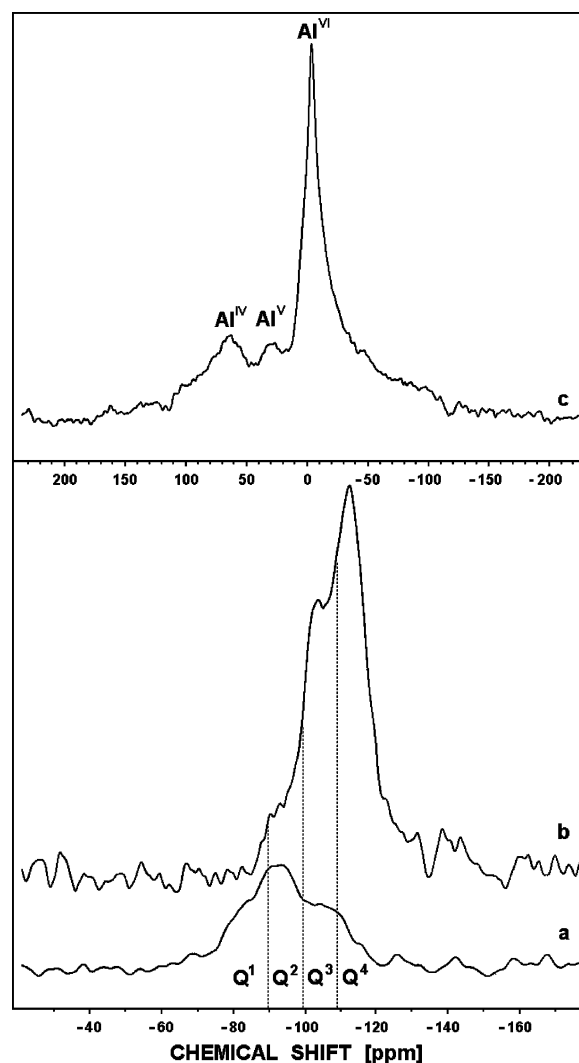

Fig. 4 ^{29}Si and ^{27}Al MAS NMR spectra of solids calcined at 893 K: (a)^{29}Si for Si-Al-Ti-Ni-Mo, (b) ^{29}Si for Si-Zr-Ti-Ni-Mo and (c) ^{27}Al for Si-Al-Ti-Ni-Mo

adsorption-desorption isotherms of Si-Zr-Ti-Ni-Mo (results not shown here) showed similar results. The pore size distribution in the mesopore zone was evaluated using the method proposed by Barret, Joiner and Halenda (BJH) [41]. The pore size distribution in the micropore zone was evaluated using the methods proposed by Horváth-Kawazoe (HK) [42], and Dubinin-Astakhov (DA). These models were used because all together they cover the full range of pore sizes. The pore size distribution of Si-Al-Ti-Ni-Mo samples appear in Fig. 6. The BET and Langmuir surface areas and the average pore diameter results appear in Table 2. Regarding the HK and DA method, the average pore diameter of the samples was found to be smaller than 2.0 nm in all cases. Finally, the densities of Si-Al-Ti-Ni-Mo and Si-Zr-Ti-Ni-Mo were 3.74 and 3.60 ± 0.01 g/cm^3, respectively. The porosity values were 40.8 and 42.5%, respectively [43].

Table 2 Porosimetry data of the Si-Al-Ti-Ni-Mo and Si-Zr-Ti-Ni-Mo samples

Sample	Temperature (K)	BET Surface Area (m²/g)	Langmuir Surface Area (m²/g)	Average Pore Diameter (nm) Method		
				BJH	HK	DA
Si-Al-Ti	423	7.94	15.9	3.25	1.42	1.76
	573	248.5	436.0	2.63	1.41	1.78
	853	156.9	794.8	3.28	1.45	1.82
	893	132.1	911.1	3.66	1.45	1.82
Si-Zr-Ti	423	59.5	105.7	3.94	1.41	1.56
	573	166.2	291.3	2.87	1.42	1.74
	853	203.4	454.1	3.09	1.42	1.82
	893	183.6	464.7	3.10	1.44	1.80
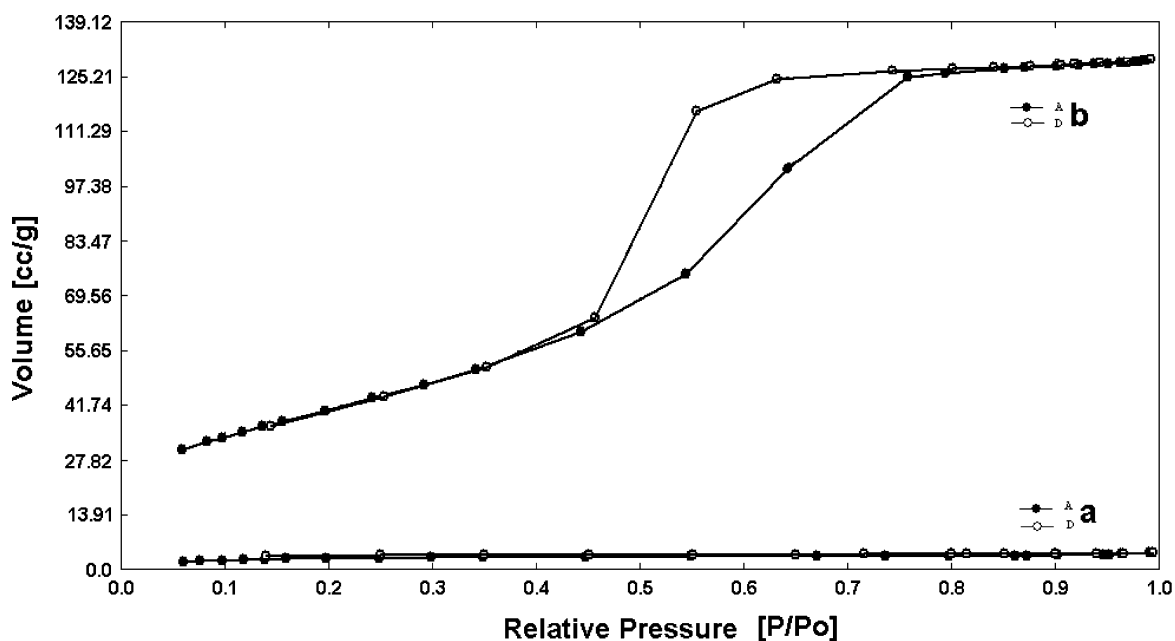
Fig. 5 Nitrogen adsorption/desorption isotherms of Si-Al-Ti-Ni-Mo at: (a) 423 K and (b) 893 K
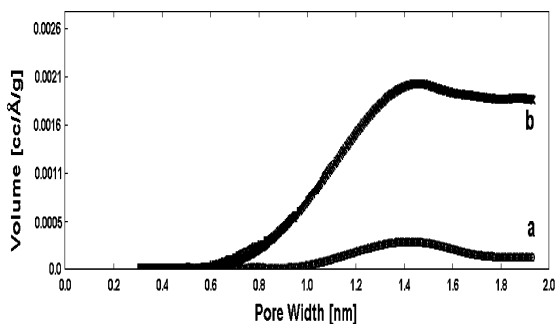
Fig. 6 Pore size distribution of Si-Al-Ti-Ni-Mo at: (a) 423 K and (b) 893 K according to the Horváth-Kawazoe model

Conclusions

The use of Al, Ti and Zr alkoxides, nickel nitrate hexahydrate, ammonium heptamolybdate tetrahydrate and the prehydrolysis of TEOS ensured the homogeneity of the sols. The polymerization process was controlled using the modifying agent acacH. The experimental strategy allowed to obtain randomly branched oligomers (Si-Al-Ti-Ni-Mo) and linear swollen polymers (Si-Zr-Ti-Ni-Mo), according to the SAXS results. The formation of the Si-O-Al, Si-O-Ni, Si-O-Ti and Si-O-Zr bands and their stability with respect to thermal treatment was demonstrated by FTIR spectroscopy. The Si-Al-Ti-Ni-Mo and Si-Zr-Ti-Ni-Mo powders analyzed by X-ray diffraction were found to be amorphous even after thermal treatment at 573 K. ^{29}Si MAS NMR indicates that different extents of condensation of the siloxane species result, depending on whether Al or Zr are incorporated. ^{27}Al MAS NMR indicated the presence in the Si-Al-Ti-Ni-Mo sample calcined at 893 K of a small amount of pentacoordinated aluminum atoms. Combined microporous and mesoporous materials were obtained in both systems.

References

1. G.S. Snow, J. Amer. Ceram. Soc. **56**(2), 91 (1973).
2. H. Perthuis, G. Velasco, and Ph. Colomban, Jap. J. Appl. Phys. **23**(5), 534 (1984).
3. M.T. Harris, A. Singhal, J.L. Look, J.R. Smith-Kristensen, J.S. Lin, and L.M. Toth, J. Sol-Gel Sci. Tech. **8**, 41 (1997).
4. G.M. Dhar, B.N. Srinivas, M.S. Rana, M. Kumar, and S.K. Maity, Catal. Today **86**, 45 (2003).
5. L.C. Klein, ed., *Sol-Gel Technology for Thin Films, Fibers, Preforms, Electronics and Specialty Shapes* (Noyes, Park Ridge. NJ, 1988).
6. A.J. Burggraaf and K. Keiser, in *Inorganic Membranes, Synthesis, Characteristics and Applications*, edited by R.R. Bhave (Van Nostrand, Reinhold. NY, 1991) p. 39.
7. R.S.A. de Lange. PhD thesis. Universiteit Twente, The Netherlands (1993).
8. C.J. Brinker, T.L. Ward, R. Sehgal, N.K. Raman, S.L. Hietala, D.M. Smith, D.-W. Hua, and T.J. Headley, J. Membrane Sci. **77**, 165 (1993).
9. J. Méndez-Vivar, R. Mendoza-Serna, P. Bosch, V.H. Lara, and C.J. Brinker, in: Proc. 4th Int. Conf. on Inorganic Membranes, Gatlinburg, TN, July 14–18, 1996.
10. Encyclopedia of catalysis, John Wiley & Sons, Inc. New York, 2002.
11. M. J. Ledoux, A. Peter, E. A. Blekkan, and F. Luck, Applied Catal. **133**, 321 (1995).
12. C.J. Brinker and G.W. Scherer, Sol-Gel Science, The Physics and Chemistry of Sol-Gel Processing (Academic Press, San Diego, CA, 1990), 839–841.
13. J.C. Debsikdar, J. Mater. Sci. **20**, 4454 (1985).
14. D. Hoebbel, T. Reinert, H. Schmidt, and E. Arpac, J. Sol-Gel Sci. Tech. **10**, 115 (1997).
15. W.C. LaCourse and S. Kim, Ceram. Eng. Sci. Proc. **8**, 1128 (1987).
16. A. Léaustic, F. Babonneau, and J. Livage, Chem. Mater. **1**, 240 (1989).
17. J.B. Miller, S.E. Rankin, and E.I. Ko, J. Catal. **148**, 673 (1994).
18. Z. Zhan and H.C. Zeng, J. Non-Cryst. Solids **243**, 26 (1999).
19. L. Valdez-Castro, J. Méndez-Vivar, and R. Mendoza-Serna, J. Porous Mater. **8**, 303 (2001).
20. O. Glatter, Acta Physica Austr. **47**, 83 (1977).
21. O. Glatter, J. Appl. Cryst. **10**, 415 (1977).
22. H.P. Klug, L.E. Alexander, *X-Ray Diffraction Procedures*, 2nd ed.; (John Wiley & Sons, NY, 1974), p. 837.
23. J. Méndez-Vivar and A. Mendoza-Bandala, J. Non-Cryst. Solids **261**, 127 (2000).
24. J. Méndez-Vivar and C.J. Brinker, J. Sol-Gel Sci. Tech. **2**, 393 (1994).
25. J. Méndez-Vivar, R. Mendoza-Serna, and L. Valdez-Castro, J. Non-Cryst. Solids **288**, 200 (2001).
26. Y. Abe, N. Sugimoto, Y. Nagao, and T. Misono, J. Non-Cryst. Solids **108**, 150 (1989).
27. T.-C. Sheng, S. Lang, B.A. Morrow, and I.D. Gay, J. Catal. **148**, 341 (1994).
28. X. Liu, C.-M. Chun, I.A. Aksay, and W-H. Shih, Ind. Eng. Chem. Res. **39**, 684 (2000).
29. Z. Congshen, H. Lisong, G. Fuxi, and J. Zhonghong, J. Non-Cryst. Solids **63**, 105 (1984).
30. J. Méndez-Vivar, P. Bosch, V.H. Lara, and R. Mendoza-Serna, J. Porous Mater. **9**, 231 (2002).
31. S. Puroit, A.P. Koley, L.S. Prasad, P.T. Manoharan, and S. Grosh, Inorg. Chem. **28**, 3735 (1989).
32. C. Rocchiccioli-Deltcheff, R. Thouvenot, and M. Fouassier, Inorg. Chem. **21**, 30 (1982).
33. C.J. Pouchert (Ed.), *The Aldrich Library of Infrared Spectra*, third ed., (Aldrich Chemical, Milwaukee, WI, 1981), p. 246.
34. Z. Liu, G.M. Crumbaugh, and R.J. Davis, J. Catal. **159**, 83 (1996).
35. L.F. Nazar and L.C. Klein, J. Am. Ceram. Soc. **71**(2), C-85 (1988).
36. S. Acosta, R. Corriu, D. Leclercq, P.H. Mutin, and A. Vioux, J. Sol-Gel Sci. Tech. **2**, 25 (1994).
37. S. Sen, and R.E. Youngman, J. Phys. Chem. B **108**, 7557 (2004).
38. S.J. Gregg and K.S.W. Sing, *Adsorption, Surface Area and Porosity*, second ed., (Academic Press, 1982), p. 195
39. S. Lowell and J.E. Shields, *Powder Surface Area and Porosity*, third ed., (Chapman & Hall, 1991), p. 11–13.
40. S.J. Gregg and K.S.W. Sing, *Adsorption, Surface Area and Porosity*, second ed., (Academic Press, 1982), p. 287.
41. E.P. Barret, L.G. Joyner, and P.P. Halenda, J. Am. Chem. Soc. **73**, 373 (1951).
42. G. Horváth and K. Kawazoe, J. Chem. Eng. Japan **16**(6), 470 (1983).
43. R.S.A. de Lange, J.H.A. Hekkink, K. Keiser, and A.J. Burggraaf, J. Non-Cryst. Solids **195**, 203 (1996).